Applied Thermal Engineering 112 (2017) 1343–1352

Contents lists available at ScienceDirect

Applied Thermal Engineering

journal homepage: www.elsevier.com/locate/apthermeng

Research Paper

A numerical study of heat transfer and pressure drop of hydrocarbon mixture refrigerant during boiling in vertical rectangular minichannel

Jiawen Yu [a], Hongqiang Ma [b], Yiqiang Jiang [a,*]

[a] School of Municipal and Environmental Engineering, Harbin Institute of Technology, Harbin 150090, China
[b] School of Civil Engineering, Lanzhou University of Technology, Lanzhou 730050, China

HIGHLIGHTS

- A model was established to investigate the characteristics of boiling heat transfer.
- The main boiling mechanism was forced convective boiling.
- The heat transfer and pressure drop increased with increasing quality and mass flux.
- The influence of heat flux was slightly for the heat transfer and pressure drop.
- An improved correlation was proposed in terms of simulation data.

ARTICLE INFO

Article history:
Received 22 May 2016
Revised 29 August 2016
Accepted 22 October 2016
Available online 24 October 2016

Keywords:
Plate fin heat exchanger
Boiling heat transfer
Friction pressure drop
Hydrocarbon mixture refrigerant
CFX

ABSTRACT

Plate-fin heat exchangers (PFHE) are probably the most common type of heat exchangers. However, studies on the heat transfer performance and pressure drop of hydrocarbon mixture refrigerant in a PFHE have rarely been conducted. In this paper, boiling heat transfer and friction pressure drop characteristics of hydrocarbon mixture refrigerant in PFHE were investigated numerically. A model was established on boiling flow in vertical rectangular minichannel, and also validated by the experiment data from literature. Results indicated that the boiling heat transfer coefficient and pressure drop increased with the increase of quality and mass flux. However, they were slightly impacted by the heat flux. This was because that the main boiling mechanism was forced convective boiling, while the effect of nucleation boiling is slight on the heat transfer. The simulation data were compared with some well-known heat transfer and pressure drop correlations. The Liu and Winterton's correlation showed the best agreement with a mean absolute deviation mostly less than ±15% for heat transfer. The calculation on Mishima and Hibiki's correlation was less than the simulated results because that the influence of heat flux was ignored for friction pressure drop in that. Meanwhile, a new correlation for pressure drop was developed with deviation less than ±15%. The presented research is helpful in designing more effective PFHE.

1. Introduction

Heat exchangers are very important during plant design and operation, and they are used extensively in process industries. Generally, plate-fin heat exchangers (PFHE) are probably the most common type of heat exchangers, which can apply for a large range of pressure and operating temperatures. Several types of PFHE are widely used in industry [1–3], including conventional gasket plate-and-frame and compact brazed shell-and-plate. In addition, they have superior thermal characteristics and high mechanical integrity [4], and are easy to manufacture under kinds of flow configurations and sizes [5]. And they usually consist of rectangular minichannels with 0.5–10 mm gap size [6]. Simultaneously, it is a key technology for the prediction on boiling heat transfer performance and friction pressure drop on hydrocarbon mixture refrigerant in rectangular minichannel for the PFHE. Unfortunately, small diameter can cause the increase of the pressure drop, which may impair the efficiency of the entire system. Therefore, the accurate heat transfer coefficient and friction pressure drop for the PFHE is very important.

Until now, the characteristic of boiling flow in the minichannel has been studied and reported by many researchers [7–12]. However, the boiling heat transfer mechanism in minichannel is still in discussions. Watel and Thonon [13] conducted boiling study with propane in a vertical serrated PFHE, and determined the effect of

* Corresponding author.
E-mail address: jyq7245@sina.com (Y. Jiang).

http://dx.doi.org/10.1016/j.applthermaleng.2016.10.151
1359-4311/

Nomenclature

A_{gl}	the interfacial area density, m^2
Bo	boiling number
C	parameter in Lockhart-Martinelli model
Co	convective number
$C_{\varepsilon 1}, C_{\varepsilon 2}, C_\mu, \sigma_K, \sigma_\varepsilon$	values for 1.44, 1.92, 0.09, 1.3, and 1.0, respectively
C_{pg}	the mixture heat capacity
C_p	specific heat at constant pressure, J kg^{-1} K^{-1}
D_h	the hydraulic diameter, m
d_{gl}	the interfacial length scale between vapor phase and liquid phase, m
E	liquid entrainment fraction
F	the factors of forced convection enhancement
f	Fanning friction factor
G	mass velocity, kg m^{-2} s^{-1}
H	the enthalpy, J kg^{-1}
H_{gs}	interfacial values of enthalpy carried into vapor phase caused by phase change
h	heat transfer coefficient, W m^{-2} K^{-1}
h_l,h_g	the heat transfer coefficient of liquid phase and vapor phase on one side of the phase interface, respectively, W m^{-2} K^{-1}
l	length of computational model, mm
M	the total of interfacial forces
$\overline{M}$	molecular mass
m	the mass flow rate, kg s^{-1}
$\dot{m}_{gl}$	the mass flow rate from liquid phase to vapor phase in per unit interfacial area, kg s^{-1}
Nu_g	a dimensionless Nusselt number in vapor phase
P	pressure, Pa
P_{kl}	the vapor phase turbulence production
P_{kbl}	the vapor phase buoyancy production term
Q	interphase sensible heat transfer to one phase across interfaces with the other phase, W
q	heat flux, W m^{-2}
r	volume fraction
S	the suppressed boiling
Su	Suratman number
T	the temperature, K
U	velocity, m s^{-1}
We	Weber number
X_{tt}	Lockhart-Martinelli parameter
x	vapor quality

Greek symbols

ε	turbulence dissipation rate
γ	the vaporization rate
Γ_{gl}	the mass flow rate from liquid phase to vapor phase in per unit volume
κ	turbulence kinetic energy
λ	thermal conductivity, W m^{-1} K^{-1}
μ	viscosity, Pa s^{-1}
μ_t	turbulent viscosity, Pa s^{-1}
ρ	density, kg m^{-3}
ϕ^2	frictional pressure gradient multiplier
σ	surface tension, N m^{-1}

Subscripts

cr	the critical condition
cl	the forced convective heat transfer in all the mass flux taken as liquid
CBD	convective boiling dominant, respectively
g, l	vapor phase and liquid phase, respectively
in	inlet
lo	liquid only
nb	the nucleation boiling in a large volume;
NBD	the nucleation boiling dominant
out	outlet
$pred$	predicted
s	interfacial
sat	the saturation condition;
sp	the forced convective
tp	two-phase

mass flux, quality, and pressure for heat transfer. They demonstrated the predominance of forced-convective boiling over nucleate boiling under the condition of different mass and heat fluxes. Contrary to their research, Palm and Claesson [14] studied the effect of various geometric parameters on heat transfer and pressure drop. Compared with the mass flux, they indicated heat transfer was governed by the heat flux during flow boiling. At the same time, Lee et al. [15] experimented the flow boiling heat transfer in PFHE under the condition of low mass flux. The results showed that the influence of convective boiling heat transfer was unobvious under given conditions, and the heat transfer coefficient increased slightly as the increase of mass flux. In addition, Choi et al. [16] examined boiling heat transfer and pressure drop of propane in horizontal minichannels. They found that the effect of mass flux on heat transfer coefficient was unobvious in the low quality. However, the heat transfer coefficient was higher under the condition of higher mass flux at the range of medium and high quality. And the heat transfer coefficient increased with the increase of saturation temperature. For the pressure drop, it was higher for high mass and heat fluxes, and it was still higher under the conditions of lower saturation temperature. They also developed new pressure drop correlation. The same conclusion could also be found by Maqbool et al. [17], who investigated the flow boiling of propane inside a vertical circular minichannel. For high mass flux, heat flux and vapor quality, the two phase frictional pressure drop gradients was higher, while it was observed reduction for higher saturation temperature.

Because of the effect of mixture physical properties estimation and mass transfer, there were significantly difference on boiling flow heat transfer with using refrigerant blends and compared to those using pure substances [18]. In addition, Wen and Ho [19] investigated heat transfer and pressure drop characteristic of R290, R600, and R290/R600 in a small-diameter tube bank. They found that the heat transfer coefficients increased with the increase of heat flux and mass flux. And the pressure drop increased with the increase of mass flux, and they proposed a new heat transfer correlation for both pure refrigerants and refrigerant mixtures. Moreover, Hsieh and Lin [20,21] studied experimentally flow boiling heat transfer and frictional pressure drop of R410a in a vertical plate heat exchanger with a hydraulic diameter of 6.6 mm. The results showed that the heat transfer coefficient and frictional pressure drop increased with the increase of heat flux, mass flux and vapor quality. In addition, under the condition of higher heat flux, the mass flux had obvious effect on the heat transfer coefficient. However, the effect of mass flux on heat transfer coefficient was unobvious at a low vapor quality.

Meanwhile, pressure drop increased more with the increase of vapor quality. They also proposed empirical correlations in terms of the equivalent Reynolds number and Boiling number.

To sum up, due to the complexity of boiling heat transfer phenomena, the boiling heat transfer mechanism in vertical rectangular minichannel is still under discussion. At the same time, a literature survey indicate that very limited research efforts have been devoted to the heat transfer and friction pressure drop on hydrocarbon mixture refrigerant in rectangular minichannel, while the heat transfer and friction pressure drop characteristics of hydrocarbon mixture refrigerant in rectangular minichannel are of significant importance to the effective design of the PFHE in petrochemical industry field. Compared with experimental, numerical simulation study has great superiority [22].

As a consequence, a numerical model was established on boiling flow heat transfer and friction pressure drop on hydrocarbon mixture refrigerant in rectangular minichannel of PFHE and validated by the experiment data from literature. In the meantime, the characteristic of boiling flow heat transfer and friction pressure drop were investigated on hydrocarbon mixture refrigerant in vertical rectangular channel. The numerical results of heat transfer coefficient and pressure drop were also compared to well known correlations. Finally, a correlation was proposed to calculate the boiling flow friction pressure drop on hydrocarbon mixture refrigerant in a vertical rectangular minichannel.

2. Numerical methods

2.1. Governing equations

Two-phase boiling process in vertical minichannel has the characteristics of thermal phase change. The governing equations are the conservation of mass and momentum, energy, and turbulent quantities. In order to calculate two phase boiling flow heat transfer, this paper used the inhomogeneous two-fluid model. During the process of flow boiling in minichannel, the mass transfer between vapor and liquid phases can be achieved by the source term of mass conservation equation, which is solved as:

$$\frac{\partial}{\partial t}(r_g\rho_g) + \nabla\cdot(r_g\rho_g U_g) = \Gamma_{gl} \tag{1}$$

$$\frac{\partial}{\partial t}(r_l\rho_l) + \nabla\cdot(r_l\rho_l U_l) = \Gamma_{lg} \tag{2}$$

where r, ρ and U, respectively, denote the volume fraction, density and velocity. Subscript g and l denote vapor phase and liquid phase, respectively. During the boiling heat transfer, Γ_{gl} is the mass flow rate that from vapor to liquid phase of per unit volume. It can be expressed as:

$$\Gamma_{gl} = A_{gl}\dot{m}_{gl} \tag{3}$$

where $\dot{m}_{gl}$ denotes the per unit interfacial area mass flow rate from vapor phase to liquid phase. A_{gl} denotes the interfacial area density between vapor and liquid phase, which can be solved by the thermal phase change model in CFX as:

$$A_{gl} = \frac{r_g r_l}{d_{gl}} \tag{4}$$

where d_{gl} represents the interfacial length scale between vapor phase and liquid phase, which can be calculated by Eq. (5):

$$d_{gl} = \sqrt{\frac{\bar{r}_g\bar{r}_l\bar{\lambda}_{gl}Nu_{gl}(1-\gamma)l}{2mx_{out}C_{pg}}} \tag{5}$$

where γ, C_{pg}, x_{out} and m represent the vaporization rate, the mixture heat capacity, the quality in outlet and the mass flow rate, respectively. According to literature [7], the γ can be written as:

$$\gamma = \frac{2(a+b)lq - abmx_{out}c_{pg}(T_{g,out}-T_{g,in})}{2(a+b)lq} \tag{6}$$

where $T_{g,out}$ and $T_{g,in}$ represent the temperature of vapor phase at outlet and inlet, respectively.

The momentum conservation equation is taken as following:

$$\begin{aligned}&\frac{\partial}{\partial t}(r_g\rho_g U_g) + \nabla\cdot\left(r_g(\rho_g U_g\otimes U_g)\right)\\ &= \nabla\cdot\left(r_g(\mu_g+\mu_{tg})(\nabla U_g + (\nabla U_g)^T)\right) - r_g\nabla p'_g\\ &\quad + r_g(\rho_g-\rho_{ref})g + M_g\end{aligned} \tag{7}$$

$$\begin{aligned}&\frac{\partial}{\partial t}(r_l\rho_l U_l) + \nabla\cdot(r_l(\rho_l U_l\otimes U_l))\\ &= \nabla\cdot\left(r_l(\mu_l+\mu_{tl})(\nabla U_l + (\nabla U_l)^T)\right) - r_l\nabla p'_l\\ &\quad + r_l(\rho_l-\rho_{ref})g + M_l\end{aligned} \tag{8}$$

where μ, μ_t and p represent, viscosity, turbulent viscosity and pressure, respectively. Operator $\otimes$ denotes a tensor product, and $(\nabla U)^T$ denotes the matrix transformation of ∇U. M represents the sum of interfacial forces.

In this paper, the turbulence model used is the standard k-ε turbulent model. For the liquid phase, the turbulent viscosity is computed from by Eq. (8):

$$\mu_{tl} = C_\mu\rho_l\frac{k_l^2}{\varepsilon_l} \tag{9}$$

where the coefficient C_μ is 0.09. κ and ε represent the turbulence kinetic energy turbulence and dissipation rate, respectively. κ and ε are obtained from Eqs. (9) and (10):

$$\frac{\partial}{\partial t}(r_l\rho_l k_l) + \nabla\cdot\left(r_l\left(\rho_l U_l k_l - \left(\mu_l + \frac{\mu_{tl}}{\sigma_k}\right)\nabla k_l\right)\right) = r_l(P_{kl}-\rho_l\varepsilon_l) \tag{10}$$

$$\frac{\partial}{\partial t}(r_l\rho_l\varepsilon_l) + \nabla\cdot\left(r_l\left(\rho_l U_l\varepsilon_l - \left(\mu_l + \frac{\mu_{tl}}{\sigma_\varepsilon}\right)\right)\nabla\varepsilon_l\right) = r_l\frac{\varepsilon_l}{k_l}(C_{\varepsilon1}P_{kl} - C_{\varepsilon2}\rho_l\varepsilon_l) \tag{11}$$

where the coefficients $C_{\varepsilon1}$, $C_{\varepsilon2}$, σ_k, and σ_ε are 1.44, 1.92, 1.0, and 1.3, respectively. P_{kl} represents the liquid phase turbulence production. It can be written as:

$$P_{kl} = \mu_{tl}\nabla U_l\cdot(\nabla U_l + \nabla U_l^T) - \frac{2}{3}\nabla\cdot U_l(3\mu_{tl}\nabla\cdot U_l + \rho_l k_l) + P_{kbl} \tag{12}$$

where P_{kbl} is the buoyancy production term for liquid phase and can be given as:

$$P_{kbl} = -\frac{\mu_{tl}}{Pr_{tl}}g\cdot\nabla\rho_\alpha \tag{13}$$

The governing equation for energy conservation can be expressed as:

$$\frac{\partial}{\partial t}(r_g\rho_g H_g) + \nabla\cdot(r_g\rho_g U_g H_g) = \nabla\cdot(r_g\lambda_g T_g) + Q_g + \Gamma_{gl}H_{gs} \tag{14}$$

$$\frac{\partial}{\partial t}(r_l\rho_l H_l) + \nabla\cdot(r_l\rho_l U_l H_l) = \nabla\cdot(r_l\lambda_l T_l) + Q_l + \Gamma_{lv}H_{ls} \tag{15}$$

where H, λ and T, respectively, denote the enthalpy, thermal conductivity and temperature. Q denotes heat transfer at the interface from one phase to the other phase. $\Gamma_{gl}H_{gs}$ and H_{gs} denote heat transfer caused by interphase mass transfer and interfacial values of enthalpy carried into vapor phase caused by phase change, respectively. Based on the thermal phase change model, the total

interphase sensible heat transfer is equal to the total heat transfer caused by interphase mass transfer, which can be written as:

$$Q_g + Q_l = -(\Gamma_{gl} H_{gs} + \Gamma_{lg} H_{ls}) \tag{16}$$

Substituting Eq. (3) in Eq. (15), the interphase mass flux $\dot{m}_{gl}$ can be written as:

$$\dot{m}_{gl} = \frac{Q_g + Q_l}{A_{gl}(H_{ls} - H_{gs})} \tag{17}$$

Based on the two resistance model in CFX, the interphase sensible heat transfer to liquid and vapor phase can be given as:

$$Q_l = h_l A_{gl}(T_s - T_l) \tag{18}$$

$$Q_g = h_g A_{gl}(T_s - T_g) \tag{19}$$

where h_l and h_g represent the heat transfer coefficient of liquid phase and vapor phase, respectively. T_s denotes the interfacial temperature, it can be determined from considerations of thermodynamic equilibrium. By ignoring effects of surface tension on pressure, the interfacial temperature can be equal to the saturation temperature T_{sat}, it can be given as:

$$T_s = T_{sat} \tag{20}$$

In this paper, zero resistance condition is used by liquid phase in the phase interface, it can force the interfacial temperature to be equal to the liquid phase temperature, $T_s = T_l$. The vapor phase heat transfer coefficient h_g can be solved by Eq. (20):

$$h_g = \frac{\lambda_g Nu_g}{d_{gl}} \tag{21}$$

where Nu_g is a dimensionless vapor phase Nusselt number.

2.2. Geometrical configurations

Plate-fin is the important component of plate-fin heat exchanger, which mainly consist of fins, plate. Due to the cyclical repeatability and complexity of plate-fin structures, some issues need to be simplified in the numerical simulation [23–26].

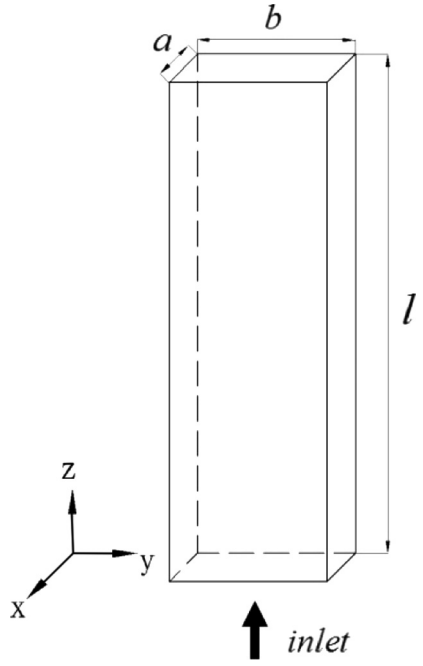

Fig. 1. Geometrical model of vertical rectangular minichannel.

The geometrical model is depicted in Fig. 1. In the orthogonal coordinate system, the Z axis represents the vertical direction, and the flow direction is upward. Inlet is set at the bottom. Cross-section dimension a × b is 1.6 × 6.3 mm and the length l is 200 mm.

2.3. Numerical method and mesh scheme

ANSYS CFX is used to investigate the characteristic of boiling flow on hydrocarbon mixture refrigerant in vertical rectangular minichannels. With a fine boundary layer mesh near the wall region, the computational domain is modeled by hexahedral cells. The mesh were created using ICEM CFD software. Three different meshes were performed in simulation: 711,000, 1,400,000 and 2,830,000 cells. Taking into account the grid-independent solution and the computation speed, the computational mesh is comprised of 1,400,000 regular hexahedral grids.

The Reynolds-averaged Navier–Stokes equations are integrated over each control volume, the mesh is used to construct finite volumes, which are used to conserve relevant quantities such as mass, momentum, and energy. The turbulence model used is the standard k-ε turbulent model. Volume integrals are discretized within each element sector and accumulated to the control volume to which the sector belongs. Discrete conservation equations are obtained by applying finite volume method, and they are assembled into the solution matrix. The diffusion terms is solved by using the central deferential scheme. Second order discretization schemes is used for the convection terms. A first order backward Euler scheme is used for the transient term. The mass flow, temperature boundary and a static pressure outlet and vapor volume fraction inlet are applied at the upstream boundary. The constant heat flux is used as the wall boundary condition. To facilitate the convergence, the steady-state solution in a vertical rectangular minichannel is obtained firstly, and then it is used as the initial condition for other cases.

3. Results and discussion

With the described above, the hydrocarbon mixture refrigerant with methane, propane and ethylene was used to study the characteristic of boiling heat transfer and frictional pressure drop in this paper. The thermo-physical properties of hydrocarbon mixture refrigerant with methane, propane and ethylene are calculated by REFPROP [26], a thermo-physical property calculation program developed by NIST.

3.1. Characteristic of boiling heat transfer

In order to validate the model used in the paper, the simulation results were compared with the experimental results from literature [2] at the different vapor quality for heat flux q = 1.1 kW/m^2, the mass flux m = 50 kg/m^2 s and heat flux q = 6 kW/m^2, the mass flux m = 215 kg/m^2 s in Fig. 2. It can be seen that simulation results and experimental data are consistent within the deviation ±15% at the different heat transfer coefficient.

Based on the model described in the previous section, the characteristic of boiling heat transfer was investigated. The influences of important parameters: vapor quality, heat flux and mass flux on the flow boiling heat transfer coefficients were discussed individually.

Fig. 3 presents heat transfer coefficient of mixture refrigerant with respect to vapor quality for the mass fluxes from 110 to 390 kg/m^2 s. In general, the heat transfer coefficients are enhanced with vapor quality increment, especially for high mass flux, which is the result of the film thickness decreasing as boiling proceeded.

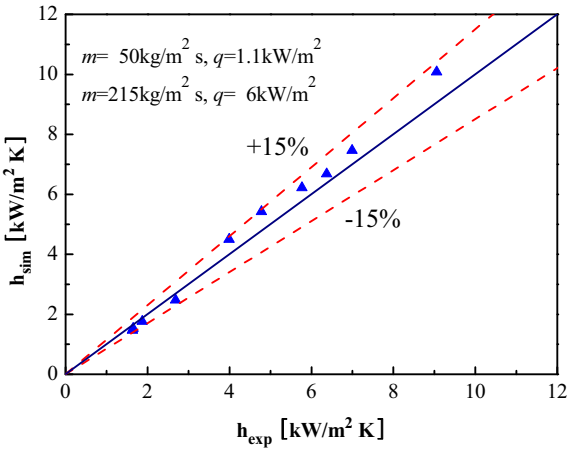

Fig. 2. Comparison between simulation results and experiment at different mass flux and heat flux.

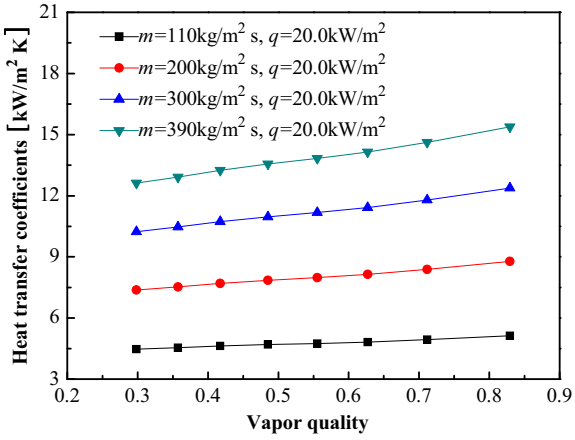

Fig. 3. The heat transfer coefficient versus vapor quality at different mass flux.

It can be explained that the decreasing liquid film thickness lead to the decrease in the thermal resistance.

Fig. 4 displays the heat transfer coefficient versus different heat flux conditions at constant mass flux, it can be observed that the heat transfer coefficients increase obviously with the increase of vapor quality. However, there are no obviously variations of the heat transfer coefficients due to the increase of heat flux in the whole range.

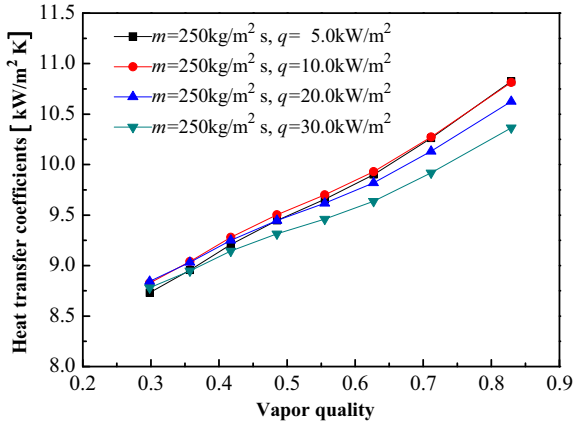

Fig. 4. The heat transfer coefficient versus vapor quality at different heat flux.

Fig. 5 displays the variation of heat transfer coefficients with mass fluxes under different vapor quality at a constant heat flux of 20 kW/m^2. The results show that the heat transfer coefficient increases with the increase of mass flux. The influence of mass flux is obvious for the heat transfer coefficient as the vapor quality increases, at the m = 390 kg/m^2 s, the heat transfer coefficient in x = 0.83 is 19% higher than that in x = 0.35. Due to an increase in shear stress at the wall and a thinning of the liquid film that decreases the boiling resistance, which results in a higher heat transfer coefficient. Meanwhile, due to the mass flux increased, the higher velocity lead to the increase of the turbulence degree of the fluid, the heat transfer coefficient is also increased.

The above results further indicate that the forced convection boiling are the main mechanisms for boiling heat transfer on hydrocarbon mixture refrigerant in minichannel. Meanwhile, the change of components and physical property of hydrocarbon mixture refrigerant is also a main influence factors.

In order to study the effect of nucleation boiling on heat transfer in a vertical rectangular minichannel, Fig. 6 displays the heat transfer coefficient versus heat flux at different mass flux and vapor quality, it shows that the heat flux has a little effect on the heat transfer coefficient, in other words, the effect of nucleation boiling is slight on the heat transfer.

An appropriate correlation is needed to examine the heat transfer coefficient for the design in engineering. At the same time, heat transfer correlations developed based on single-component

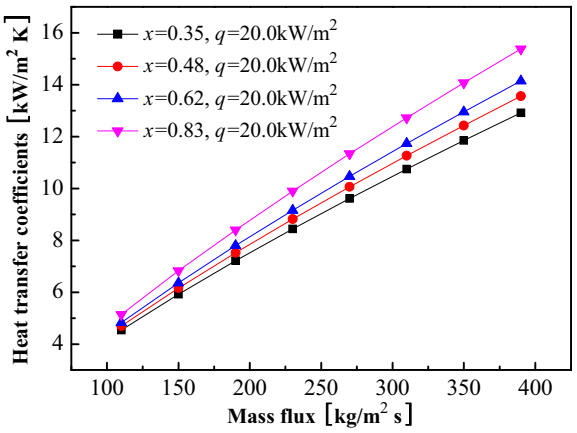

Fig. 5. The heat transfer coefficient versus mass flux at different vapor quality.

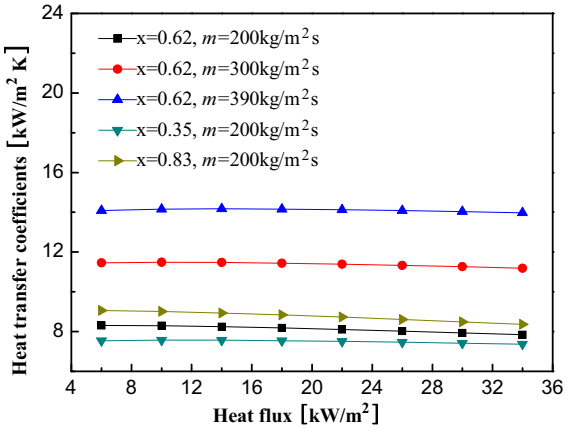

Fig. 6. The heat transfer coefficient versus heat flux at different mass flux and vapor quality.

Table 1
Description of correlation for boiling heat transfer coefficient.

Authors	Heat transfer coefficient correlation
Tran [27]	$h_{tp} = 8.4 \times 10^5 (Bo \times We_{lo})^{0.3} (\frac{\rho_g}{\rho_l})^{0.4}$, $We_{lo} = \frac{G^2 D_h}{\rho_l \sigma}$
Bertsch [28]	$h_{tp} = E \cdot h_{sp} + S \cdot h_{nb}$, $E = 1 + 80(x^2 - x^6)e^{-0.6Co}$ $S = f(x) = 1 - x$, $h_{sp} = h_{conv,l}(1-x) + h_{conv,v}x$ $h_{nb} = 55 P_r^{0.12} (-\log_{10} P_r)^{-0.55} M^{-0.5} (q)^{\frac{2}{3}}$ $h_{conv,l} = \frac{k_l}{D_h}\left(3.66 + \frac{0.0668 \frac{D_h}{L} Re_{lo} Pr_l}{1+0.04\left[\frac{D_h}{L} Re_{lo} Pr_l\right]^{2/3}}\right)$
Gungon [29]	$h_{tp} = E \cdot h_{sp} + S \cdot h_{nb}$, $E = 1 + 24000 Bo^{1.16} + 1.37(\frac{1}{X})^{0.86}$ $S = (1 + 1.15 \times 10^{-6} E^2 Re_l^{1.17})^{-1}$, $h_{sp} = 0.023 Re_l^{0.8} Pr^{0.4} \frac{k_l}{D_h} h_{nb} = 55 P_r^{0.12} (-\log_{10} P_r)^{-0.55} M^{-0.5} (q)^{\frac{2}{3}}$
Liu and Winterton [1]	$h_{tp}^2 = (F h_{cl})^2 + (S h_{nb})^2$, $F = \left[1 + xPr_l(\frac{\rho_L}{\rho_v} - 1)\right]^{0.35}$ $S = (1 + 0.055 F^{0.1} Re_{lo}^{0.16})^{-1}$, $h_{cl} = 0.023 Re_l^{0.8} Pr^{0.4} \frac{k_l}{D_h}$ $h_{nb} = 550 P_{cr}^{0.25} T_{cr}^{-0.875} M^{-0.125} q^{0.75} R_z^{0.2} \left(0,14 + 2.2 \frac{P}{P_{cr}}\right)$

refrigerant needs deep comparison and analysis. The applicability to predict heat transfer coefficients for hydrocarbon mixture refrigerant in vertical rectangular minichannel needs further evaluation. Therefore, the simulation results were compared with the predicted results of well known heat transfer coefficients correlations at the temperature T = 150–215 K, pressure P = 0.2–0.5 MPa, mass flux m = 100–400 kg/m^2 s and heat flux q = 5–20 kW/m^2. The correlations used in this paper were listed in Table 1.

The comparisons of the simulation results and correlation are shown in Fig. 7.

The simulated boiling heat transfer coefficient were compared with the Tran et al. [27] calculations as shown in Fig. 7(a). They correlated heat transfer coefficients by using a Weber number. The results show that the simulation results are slightly underpredicted. The deviations are less than 15% in most cases. Fig. 7(b) shows that the correlation by the Bertsch et al. [28] are less than the simulation results with the deviations more than −15% in most cases. They show relatively poor agreement with the simulation results. At high values of heat transfer coefficient, the correlation under predicts the simulation data, however, it shows good predictions at medium and lower heat transfer coefficient. Fig. 7 (c) indicates that the correlation by Gungor and Winterton [29] accords with the simulation results in some cases, but the deviations between the simulation results and correlation calculations are still more than 15% in many cases. It is still very difficult to use Tran, Bertsch and Gungon correlation accurately to predict the heat transfer coefficient on the boiling heat transfer of hydrocarbon mixture refrigerant in vertical rectangular minichannel.

Liu and Winterton [1] presented a correlation by considering nucleate and convective boiling. As shown in Fig. 7(d), the simulation results with the deviations fall within ±15% in most cases, and its predicted result among the correlations is the most accurate.

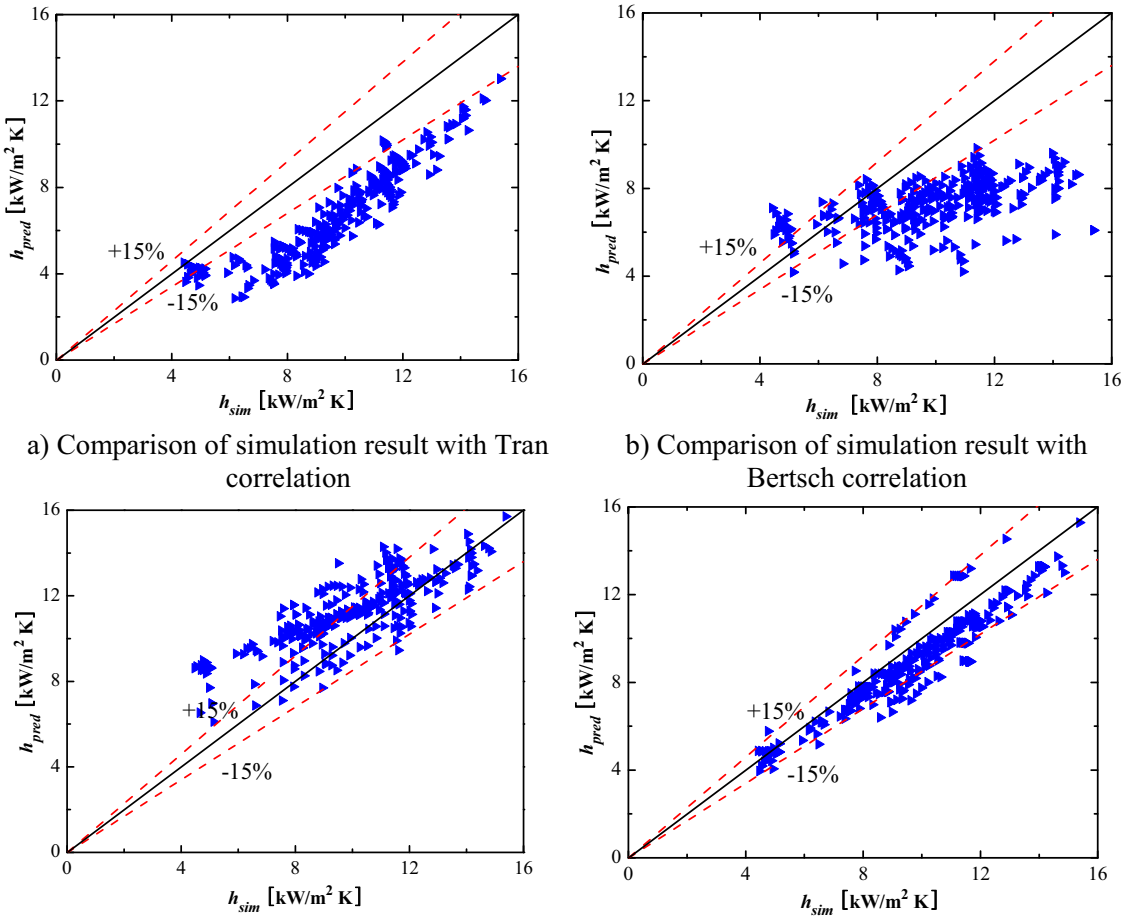

a) Comparison of simulation result with Tran correlation

b) Comparison of simulation result with Bertsch correlation

c) Comparison of simulation result with Gungon correlation

d) Comparison of simulation result with Liu and Winterton correlation

Fig. 7. Comparison of heat transfer coefficient with other correlations.

3.2. Pressure drop

To predict boiling flow friction pressure drop of hydrocarbon mixture refrigerant in the PFHE, in this section, the characteristic of friction pressure drop change of hydrocarbon mixed refrigerant boiling flow was simulated.

Fig. 8 displays the frictional pressure drop versus vapor quality at different mass flux and constant heat flux. The frictional pressure drop increases with the increase of mass flux for a certain vapor quality. And it also increases with the increase of vapor quality. It can be explained that the higher vapor velocity caused by high vapor quality can generate shear stress at the interface of the film. Furthermore, at equal vapor quality, the higher mass flux will lead to a higher vapor velocity and degree of flow turbulence, which can increase the shear stress of interface. therefore, the frictional pressure drop is increased.

The effect of heat flux on the frictional pressure drop of boiling is shown in Fig. 9. It shows that the frictional pressure drop increases with the increase of vapor quality at different heat flux, however, the pressure drop is not obvious with the increase of heat flux.

Fig. 10 displays the variation of pressure drop versus different mass fluxes at average vapor quality. It can be seen that the frictional pressure drop increases with the increase of the vapor quality for all mass fluxes. The increase of pressure drop is obvious under the high vapor quality. At the m = 390 kg/m^2 s, the pressure drop in x = 0.83 is 83% higher than that in x = 0.35. It can be explain that the higher vapor phase flows can increase the degree of turbulence, and lead to a higher interfacial vapor liquid shear stress, therefore, pressure drop is increased.

To investigate the effect of heat flux on frictional pressure drop, as shown in Fig. 11, different values of heat flux were investigated in the paper. Fig. 11 represents the relationship between pressure drop and heat flux at constant values of mass flux and vapor quality respectively. It can be seen that the heat flux has little effect on the pressure drop in the whole simulation range.

In this paper, the simulated frictional pressure drops results were compared against four correlations of Mishima and Hibiki [30], Souza and Pimenta [31], Kim and Mudawar [32], Chen et al. [33]. Based on our simulation data, a new correlation for pressure drop was developed. As list in Table 2.

Fig. 12 presents the comparison of the simulation frictional pressure drop data with the prediction models.

The prediction of the Mishima and Hibiki [30] correlation is shown in Fig. 12a. It shows good predictions of experimental pressure drop data with the deviations mostly falling within ±15%. Fig. 12b shows the experimental frictional pressure drops compared with the correlation of Souza and Pimenta [31]. It can be seen that the correlation over predicts the simulation data at high pressure drops and the deviations is more than that of Mishima and Hibiki [30] correlation. Fig. 12c shows the experimental frictional pressure drops compared with the correlation of Kim and Mudawar [32], based on the Lockhart and Martinelli [34] correlation, this correlation has a modified values of C (Chisholm's

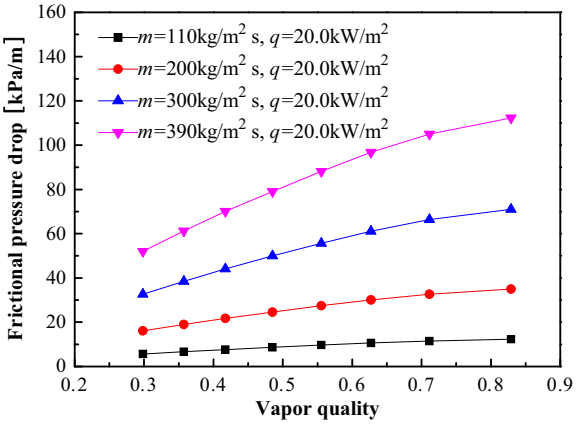

Fig. 8. The frictional pressure drop versus vapor quality at different mass flux.

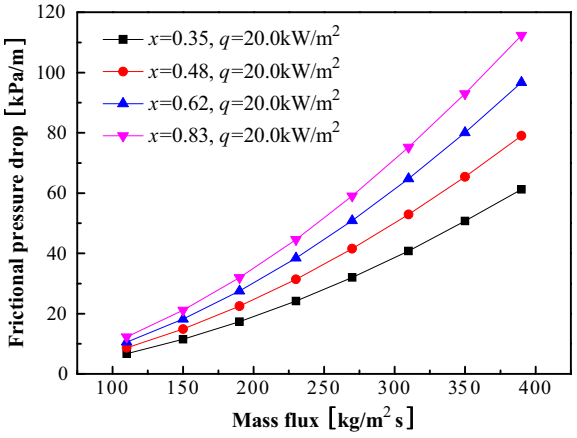

Fig. 10. The frictional pressure drop versus mass flux at different vapor quality.

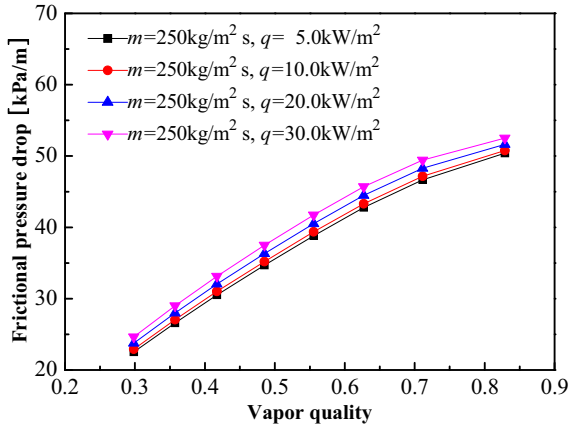

Fig. 9. The frictional pressure drop versus vapor quality at different heat flux.

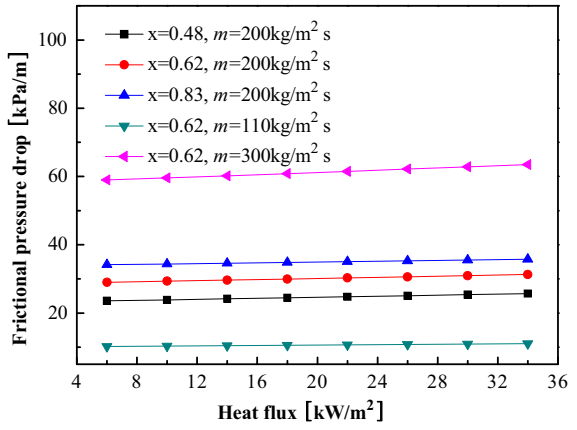

Fig. 11. The frictional pressure drop versus heat flux at different mass flux and vapor quality.

Table 2
Description of correlation for frictional pressure drop.

Authors	Frictional pressure drop correlation
Mishima and Hibiki [30]	$(dp/dz)_{f,tp}=\phi_l^2(dp/dz)_l$, $(dp/dz)_l=-2f_l\left[m^2(1-x)^2/(\rho_l D_h)\right]$ $f_l=0.079Re_l^{-0.25}$, $\phi_l^2=1+C/X+1/X^2$, $C=21(1-e^{-319D_h})$
Souza and Pimenta [31]	$\phi_{lo}^2=1+(\Gamma^2-1)x^{1.75}\left(1+0.9524\Gamma X_{tt}^{0.4126}\right)$, $\Gamma=\left(\frac{\rho_l}{\rho_g}\right)^{0.5}\left(\frac{\mu_g}{\mu_l}\right)^{0.125}$ $X_{tt}=\frac{1}{\Gamma}\left(\frac{1-x}{x}\right)^{0.875}$
Kim [32]	$(dp/dz)_{f,tp}=\phi_l^2(dp/dz)_l$, $(dp/dz)_l=-2f_l\left[m^2(1-x)^2/(\rho_l D_h)\right]$, $\phi_l^2=1+C/X+1/X^2$, $f_l=\begin{cases}16Re_l^{-1}, Re_l<2000\\ 0.079Re_l^{-0.25}, 2000<Re_l<20000\\ 0.046Re_l^{-0.2}, Re_l>20000\end{cases}$. $C_{boiling}=C_{non-boiling}\times\begin{cases}1+60[(m^2D_h)/(\rho_l\sigma)]^{0.32}(Bo)^{0.78}, Re_l\geqslant 2000\\ 1+530[(m^2D_h)/(\rho_l\sigma)]^{0.52}(Bo)^{1.09}, Re_l<2000\end{cases}$ $C_{non-boiling}=\begin{cases}0.39Re_{lo}^{0.03}Su_{go}^{0.10}(\rho_l/\rho_g)^{0.35}, & Re_l\geqslant 2000, Re_g\geqslant 2000\\ 8.7\times10^{-4}Re_{lo}^{0.17}Su_{go}^{0.50}(\rho_l/\rho_g)^{0.14}, & Re_l\geqslant 2000, Re_g<2000\\ 0.0015Re_{lo}^{0.59}Su_{go}^{0.19}(\rho_l/\rho_g)^{0.36}, & Re_l<2000, Re_g\geqslant 2000\\ 3.5\times10^{-5}Re_{lo}^{0.44}Su_{go}^{0.50}(\rho_l/\rho_g)^{0.48}, & Re_l<2000, Re_g<2000\end{cases}$
Chen [33]	$(dp/dz)_{f,tp}=\Omega(dp/dz)_{tp,Friedel}$, $(dp/dz)_{tp,Friedel}=\phi_{lo}^2(dp/dz)_{lo}$ $(dp/dz)_{lo}=-2f_{lo}[G^2/(\rho_l D_h)]$, $f_{lo}=0.079Re^{-0.25}$ $\phi_{lo}^2=E+\left[3024FX/(Fr_{tp}^{0.045}We_l^{0.035})\right]$, $Fr_{tp}=G^2/(gD_h\rho_{tp}^2)$ $We_l=G^2D_h/(\sigma\rho_{tp})$ $1/\rho_{tp}=x/\rho_g+(1-x)/\rho_l$, $\Omega=\begin{cases}0.0333Re_{lo}^{0.45}Re_g^{-0.09}[1+0.4\exp(-Bo)]^{-1}, Bo<2.5\\ We_{tp}^{0.2}(2.5+0.06Bo)^{-1}, Bo\geqslant 2.5\end{cases}$
New correlation	$(dp/dz)_{f,tp}=\phi_l^2(dp/dz)_l$, $(dp/dz)_l=-2f_lm^2(1-x)^2/(\rho_l D_h)f_l=0.079Re_l^{-0.25}$, $\phi_l^2=1+C/X+1/X^2$ $C=21(1-e^{-319D_h})\times\begin{cases}1+60[(m^2D_h)/(\rho_l\sigma)]^{0.32}(Bo)^{0.78}, & Re_l\geqslant 2000\\ 1+530[(m^2D_h)/(\rho_l\sigma)]^{0.52}(Bo)^{1.09}, & Re_l<2000\end{cases}$

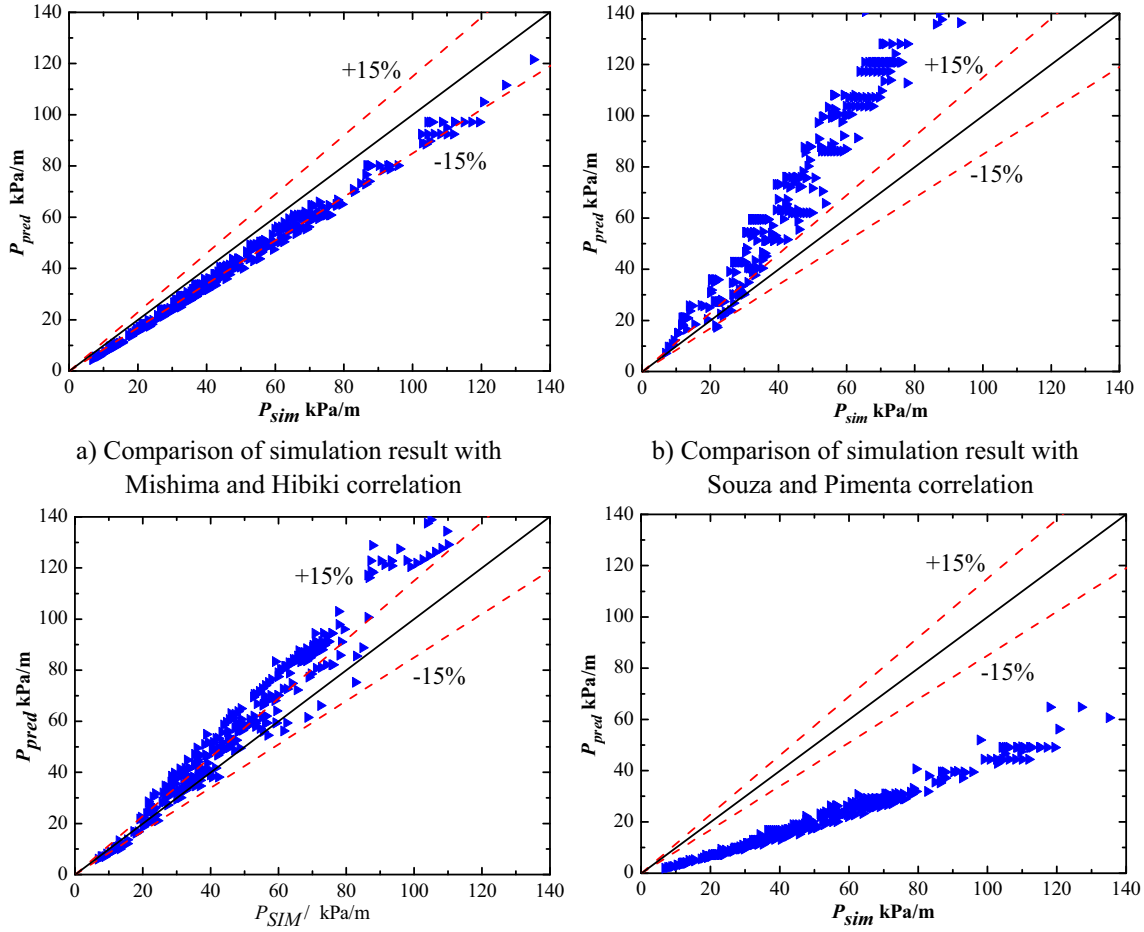

a) Comparison of simulation result with Mishima and Hibiki correlation

b) Comparison of simulation result with Souza and Pimenta correlation

c) Comparison of simulation result with Sung -Min Kim correlation

d) Comparison of simulation result with Chen correlation

Fig. 12. Comparison of frictional pressure drop with other correlations.

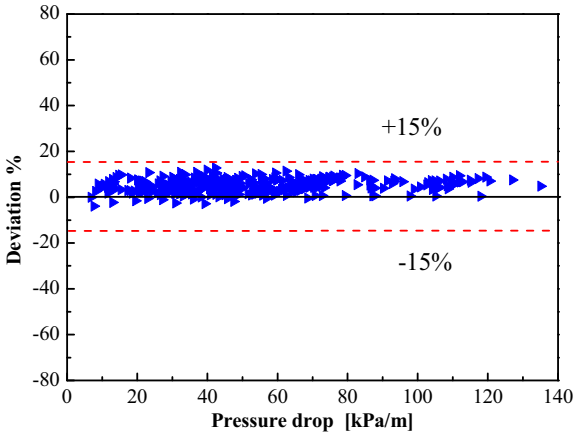

Fig. 13. Comparison of frictional pressure drop with new correlation.

parameter). It can be seen from the figure that the correlation has a good prediction at low frictional pressure drops, while has a poor prediction for most conditions. Fig. 12d shows the experimental frictional pressure drops compared with the correlation of Chen et al. [33]. The results show that the present heat transfer coefficients are strongly underestimated by the Chen model.

In the two-phase flow, the frictional pressure drop gradient is correlated by the relationship between the two-phase frictional multiplier, ϕ_l^2 and X, for smooth circular tube, the two-phase frictional multiplier can be written in form of Lockhart–Martinelli correlation as:

$$\phi_l^2 = 1 + C/X + 1/X^2 \tag{22}$$

The constant C indicates the two-phase flow condition parameter in the Eq. (21).

Based on above discussion and Mishima and Hibiki [30] correlation. A new correlation is proposed in this paper:

$$(dp/dz)_{f.tp} = \phi_l^2 (dp/dz)_l \tag{23}$$

$$(dp/dz)_l = -2f_l m^2 (1-x)^2/(\rho_l D_h) \tag{24}$$

$$f_l = 0.079 Re_l^{-0.25} \tag{25}$$

$$C = 21(1 - e^{-319 D_h}) \times \begin{cases} 1 + 60\left[(m^2 D_h)/(\rho_l \sigma)\right]^{0.32} (Bo)^{0.78}, & Re_l \geqslant 2000 \\ 1 + 530\left[(m^2 D_h)/(\rho_l \sigma)\right]^{0.52} (Bo)^{1.09}, & Re_l < 2000 \end{cases} \tag{26}$$

Fig. 13 compares the present frictional pressure drop data with predictions of the new correlation, Eqs. (21)–(25), which shows best predictions of the simulation data. The whole deviation is shown within ±15%.

4. Conclusions

In this paper, a model was established to investigate the characteristic of frictional pressure drop for hydrocarbon mixture refrigerant in vertical rectangular minichannel. The effect of mass flux, vapor quality and heat flux on heat transfer coefficients and pressure drop gradients were discussed. And the simulation results were compared with the existing correlations of heat transfer coefficient and frictional pressure drop developed in literatures. The following conclusions can be drawn from this study.

(1) The simulation results and experimental data from the literatures are consistent within the deviation ±15% at the different heat transfer coefficient.
(2) Due to the influence of the forced convection boiling mechanisms, the heat transfer coefficient increased with the increase of vapor quality and the mass flux, while the influence of heat flux was found to be insignificant.
(3) Frictional pressure drop gradients increased with the increase of vapor quality and mass flux, and the heat flux had a little effect on the frictional pressure drop.
(4) The simulation results of heat transfer coefficients and pressure drop were compared to existing correlations, the heat transfer coefficient model of Liu correlation can predict most of simulation data with the deviations in ±15%. Muller-Steinhagen and Heck correlation show good predictions of experimental pressure drop data with the deviations mostly falling within ±15%. The modified model for frictional pressure gradients shows the best prediction ability.

Acknowledgements

This work was supported by the research funds from High Technology Ship Scientific Research Program by Ministry of Industry and Information Technology of the people's Republic of China, No. ([2012]534).

References

[1] Z. Liu, R. Winterton, A general correlation for saturated and subcooled flow boiling in tubes and annuli, based on a nucleate pool boiling equation, Int. J. Heat Mass Transfer 34 (1991) 2759–2766.
[2] V.V. Kuznetsov, A.S. Shamirzaev, Boiling heat transfer for freon R21 in rectangular minichannel, Heat Transfer Eng. 28 (2007) 738–745.
[3] W.C. Jiang, J.M. Gong, S.T. Tu, H. Chen, Effect of geometric conditions on residual stress of brazed stainless steel plate-fin structure, Nucl. Eng. Des. 238 (2008) 1497–1502.
[4] Z.H. Ayub, Plate heat exchanger literature survey and new heat transfer and pressure drop correlations for refrigerant evaporators, Heat Transfer Eng. 24 (2003) 3–16.
[5] H. Peng, X. Ling, Optimal design approach for the plate-fin heat exchangers using neural networks cooperated with genetic algorithms, Appl. Therm. Eng. 28 (2008) 642–650.
[6] W.C. Jiang, J.M. Gong, S.D. Tu, Q.S. Fan, A comparison of brazed residual stress in plate-fin structure made of different stainless steel, Mater. Des. 30 (2009) 23–27.
[7] H. Ma, W. Cai, J. Chen, Y. Yao, Y. Jiang, Numerical investigation on saturated boiling and heat transfer correlations in a vertical rectangular minichannel, Int. J. Therm. Sci. 102 (2016) 285–299.
[8] D. Del Col, M. Bortolato, S. Bortolin, Comprehensive experimental investigation of two-phase heat transfer and pressure drop with propane in a minichannel, Int. J. Refrig. 47 (2014) 66–84.
[9] W. Cai, H. Ma, Y. Yao, Y. Jiang, Numerical investigation on saturated boiling heat transfer in a vertical rectangular minichannel, in: ASME/JSME/KSME 2015 Joint Fluids Engineering Conference, 2015.
[10] Y.Y. Yan, T.F. Lin, Evaporation heat transfer and pressure drop of refrigerant R-134a in a plate heat exchanger, J. Heat Transfer 121 (1999) 118–127.
[11] W. Tong, A.E. Bergles, M.K. Jensen, Pressure drop with highly subcooled flow boiling in small-diameter tubes, Exp. Thermal Fluid Sci. 15 (1997) 202–212.
[12] G.M. Lazarek, S.H. Black, Evaporative heat transfer, pressure drop and critical heat flux in a small vertical tube with R-113, Int. J. Heat Mass Transfer 25 (1982) 945–960.
[13] B. Watel, B. Thonon, An experimental study of convective boiling in a compact serrated plate-fin heat exchanger, J. Enhanced Heat Transfer 9 (2002) 1–15.
[14] B. Palm, J. Claesson, Plate heat exchangers: calculation methods for single and two-phase flow, Heat Transfer Eng. 27 (2006) 88–98.
[15] H. Lee, S. Li, Y. Hwang, R. Radermacher, H.-H. Chun, Experimental investigations on flow boiling heat transfer in plate heat exchanger at low mass flux condition, Appl. Therm. Eng. 61 (2013) 408–415.
[16] K.-I. Choi, A.S. Pamitran, J.-T. Oh, K. Saito, Pressure drop and heat transfer during two-phase flow vaporization of propane in horizontal smooth minichannels, Int. J. Refrig. 32 (2009) 837–845.
[17] M.H. Maqbool, B. Palm, R. Khodabandeh, Investigation of two phase heat transfer and pressure drop of propane in a vertical circular minichannel, Exp. Thermal Fluid Sci. 46 (2013) 120–130.
[18] K. Stephan, Two-phase heat exchange for new refrigerants and their mixtures, Int. J. Refrig. 18 (1995) 198–209.

[19] M.-Y. Wen, C.-Y. Ho, Evaporation heat transfer and pressure drop characteristics of R-290 (propane), R-600 (butane), and a mixture of R-290/R-600 in the three-lines serpentine small-tube bank, Appl. Therm. Eng. 25 (2005) 2921–2936.
[20] Y.Y. Hsieh, T.F. Lin, Saturated flow boiling heat transfer and pressure drop of refrigerant R-410A in a vertical plate heat exchanger, Int. J. Heat Mass Transfer 45 (2002) 1033–1044.
[21] Y.Y. Hsieh, T.F. Lin, Evaporation heat transfer and pressure drop of refrigerant R-410A flow in a vertical plate heat exchanger, J. Heat Transfer 125 (2003) 852–857.
[22] M.A. Jemni, G. Kantchev, M.S. Abid, Influence of intake manifold design on in-cylinder flow and engine performances in a bus diesel engine converted to LPG gas fuelled, using CFD analyses and experimental investigations, Energy 36 (2011) 2701–2715.
[23] H. Ma, W. Cai, Y. Yao, Y. Jiang, Investigation on stress characteristics of plate-fin structures in the heat-up process of LNG heat exchanger, J. Nat. Gas Sci. Eng. 30 (2016) 256–267.
[24] H. Ma, W. Cai, W. Zheng, J. Chen, Y. Yao, Y. Jiang, Stress characteristics of plate-fin structures in the cool-down process of LNG heat exchanger, J. Nat. Gas Sci. Eng. 21 (2014) 1113–1126.
[25] H. Ma, J. Chen, W. Cai, C. Shen, Y. Yao, Y. Jiang, The influence of operation parameters on stress of plate-fin structures in LNG heat exchanger, J. Nat. Gas Sci. Eng. 26 (2015) 216–228.
[26] E.W. Lemmon, M.L. Huber, M.O. Mclinden, NIST Standard Reference Database 23: Reference Fluid Thermodynamic and Transport Properties-REFPROP. 9.0, 2010.
[27] T.N. Tran, M.W. Wambsganss, D.M. France, Small circular- and rectangular-channel boiling with two refrigerants, Int. J. Multiph. Flow 22 (1996) 485–498.
[28] S.S. Bertsch, E.A. Groll, S.V. Garimella, A composite heat transfer correlation for saturated flow boiling in small channels, Int. J. Heat Mass Transfer 52 (2009) 2110–2118.
[29] K.E. Gungor, R.H.S. Winterton, A general correlation for flow boiling in tubes and annuli, Int. J. Heat Mass Transfer 29 (1986) 351–358.
[30] K. Mishima, T. Hibiki, Some characteristics of air-water two-phase flow in small diameter vertical tubes, Int. J. Multiph. Flow 22 (1996) 703–712.
[31] A. Lobo de Souza, M. de Mattos Pimenta, Prediction of pressure drop during horizontal two-phase flow of pure and mixed refrigerants, ASME-PUBLICATIONS-FED, 210, 1995, pp. 161–172.
[32] S.-M. Kim, I. Mudawar, Universal approach to predicting two-phase frictional pressure drop for mini/micro-channel saturated flow boiling, Int. J. Heat Mass Transfer 58 (2013) 718–734.
[33] I.Y. Chen, K.-S. Yang, Y.-J. Chang, C.-C. Wang, Two-phase pressure drop of air–water and R-410A in small horizontal tubes, Int. J. Multiph. Flow 27 (2001) 1293–1299.
[34] R. Lockhart, R. Martinelli, Proposed correlation of data for isothermal two-phase, two-component flow in pipes, Chem. Eng. Prog. 45 (1949) 39–48.